Manuscript Details

Manuscript number	JTEMB_2017_539_R2
Title	Rough and tough. How does silicic acid protect horsetail from fungal infection?
Article type	Research Paper

Abstract

Horsetail (Equisetum arvense) plants grew healthily for 10 weeks under both Si-deficient and Si-replete conditions. After 10 weeks, plants grown under Si-deficient conditions succumbed to fungal infection. We have used NanoSIMS and fluorescence microscopy to investigate silica deposition in the tissues of these plants. Horsetail grown under Si-deficient conditions did not deposit identifiable amounts of silica in their tissues. Plants grown under Si-replete conditions accumulated silica throughout their tissues and especially in the epidermis of the outer side of the leaf and the furrow region of the stem where it was continuous and often, as a double layer suggestive of a barrier function. We have previously shown, both in vivo (in horsetail and thale cress) and in vitro (using an undersaturated solution of Si(OH)4), that callose is a “catalyst” of plant silica deposition. Here we support this finding by comparing the deposition of silica to that of callose and by showing that they are co-localized. We propose the existence of a synergistic mechanical protection by callose and silica against pathogens in horsetail, whereby the induction of callose synthesis and deposition is the first, biochemical line of defence and callose-induced precipitation of silica is the second, adventitious mechanical barrier.

Keywords	Biogenic silica; NanoSIMS; Silicic acid; Callose; Horsetail; Fungal infection.
Manuscript category	Bioinorganic chemistry

Corresponding Author	Christopher Exley
Corresponding Author's Institution	Keele University
Order of Authors	Gea Guerriero, Chinnoi Law, Ian Stokes, Katie Moore, Christopher Exley

Suggested reviewers	Lu Shin Wong, Adriana Basile

Submission Files Included in this PDF

File Name [File Type]

Cover Letter JTEMB Final.docx [Cover Letter]

Reply to Reviewer 3 JTEMB_2017_539_R1.docx [Response to Reviewers]

JTEMB Final Revised ms GG_second round.docx [Manuscript File]

Figure 1 JTEMB.tif [Figure]

Figure 2 JTEMB.tif [Figure]

Figure 3 JTEMB.tif [Figure]

Figure 4 JTEMB.tif [Figure]

Figure 5 JTEMB.tif [Figure]

Figure 6 JTEMB.tif [Figure]

Figure 7 JTEMB.tif [Figure]

Figure 8 JTEMB.tif [Figure]

Competing interests.docx [Conflict of Interest]

To view all the submission files, including those not included in the PDF, click on the manuscript title on your EVISE Homepage, then click 'Download zip file'.

Rough and tough. How does silicic acid protect horsetail from fungal infection?

Gea Guerriero[1], Chinnoi Law[2], Ian Stokes[2], Katie L Moore[3] and Christopher Exley[2,*]

[1]Environmental Research and Innovation Department, Luxembourg Institute of Science and Technology, Esch/Alzette, Luxembourg.

[2]The Birchall Centre, Lennard-Jones Laboratories, Keele University, Stoke-on-Trent, UK.

[3]School of Materials and Photon Science Institute, University of Manchester, Oxford Road, Manchester, UK.

***Correspondence**

Prof. Christopher Exley

The Birchall Centre

Lennard-Jones Laboratories

Keele University

Staffordshire, ST5 5BG, UK.

E-mail: c.exley@keele.ac.uk

Telephone: +44 1782 734080

Keywords: Biogenic silica, NanoSIMS, Silicic acid, Callose, Horsetail, Fungal infection.

Abstract

Horsetail (*Equisetum arvense*) plants grew healthily for 10 weeks under both Si-deficient and Si-replete conditions. After 10 weeks, plants grown under Si-deficient conditions succumbed to fungal infection. We have used NanoSIMS and fluorescence microscopy to investigate silica deposition in the tissues of these plants. Horsetail grown under Si-deficient conditions did not deposit identifiable amounts of silica in their tissues. Plants grown under Si-replete conditions accumulated silica throughout their tissues and especially in the epidermis of the outer side of the leaf and the furrow region of the stem where it was continuous and often, as

a double layer suggestive of a barrier function. We have previously shown, both *in vivo* (in horsetail and thale cress) and *in vitro* (using an undersaturated solution of $Si(OH)_4$), that callose is a "catalyst" of plant silica deposition. Here we support this finding by comparing the deposition of silica to that of callose and by showing that they are co-localized. We propose the existence of a synergistic mechanical protection by callose and silica against pathogens in horsetail, whereby the induction of callose synthesis and deposition is the first, biochemical line of defence and callose-induced precipitation of silica is the second, adventitious mechanical barrier.

1. Introduction

Silicon is a non-essential element for plants, as its presence is not required for the completion of their life cycle. Nevertheless, silicon improves plant vigour and resistance to biotic and abiotic stressors [1]. Plants take up silicon in the form of silicic acid, $Si(OH)_4$, deposit it as biogenic silica and are classified according to their propensities to accumulate it in their tissues. Horsetail and the commelinoid monocot rice are emblematic examples of highly silicifying plants (accumulating up to 10% silica by dry weight), while tomato is an excluder [2]. The association of biogenic silica with plant cell walls provides mechanical defence against pathogens [3] and is a deterrent against phytophagous insects [4].

A role for cell wall mixed-linkage glucans in biosilicification was shown in both horsetail [5] and rice [6]. In rice, the overexpression of a (1;3,1;4)-β-D-glucanase impacted the mechanical properties of the leaf blade and altered the distribution profile of silica [6]. In horsetail, it was demonstrated *in vivo* that silica accumulation mirrored callose deposition [7]. Importantly, this result was validated *in vitro*, where callose catalysed the precipitation of amorphous silica from an undersaturated solution of silicic acid [7]. Further support for a role of callose in templating silica deposition came in the non-Si accumulator thale cress, where mutants

lacking the callose synthase gene *PMR4* showed significantly less silica deposition than either wild type or plants over-expressing this gene [8].

Using mild extraction procedures where silica was released from cell walls, silica was proposed to be involved in enhanced mechanical rigidity/stability against (a)biotic stresses in *Equisetum arvense* [9].

In this study, we provide evidence for the existence of a continuous silica layer in *E. arvense* tissues (double in specific regions), using for the first time NanoSIMS and propose a synergistic role with callose protecting against biotic stress.

2. Materials and Methods

2.1 Hydroponic culture

Horsetail plants were collected, locally, from the wild in the early spring. Each plant had ca 3cm of intact basal stem associated with the roots. The roots of washed plants were submerged in 20mL of 1/6 Murashige Skoog (MS) basal salt growth solution (Sigma Aldrich M5524) at pH 5.8. The growth solutions were controlled to contain either 2mM silicic acid (Alfa Aesar, Na_4SiO_4, Mw184), referred to as Si-replete, or 8mM sodium (AnalaR BDH Labs, NaOH, Mw 40) referred to as Si-deficient. The growth environment consisted of ca 14h light/10h dark, at 25°C. The growth solutions were replenished every other day. Plants were grown under these conditions for 12 weeks. The total Si content of the Si-deficient treatment was 12μM as measured by TH GFAAS [7].

2.2 Preparation of plant tissues for PDMPO fluorescence

Horsetail samples were separated according to their anatomical region of basal stem, distal stem, leaves, nodes and root. Samples were cut with small scissors to a length of 1cm. The samples (<0.5g) were digested in PFA Teflon© vessels with venting plugs and screw caps (CEM Microwave Technology Ltd, UK) using a 1:1 mixture of 15.8M HNO_3 and 18.4M

H_2SO_4. Vessels were placed in insulating sleeves on a turntable, capable of holding up to 40 vessels. The microwave digestion programme was set up with Mars Xpress Microwave (CEM Microwave Technology Ltd, UK) using a CEM-provided Tissue Express organics method. Digested samples were diluted with ultrapure water (cond. <0.067µS/cm) and silica was collected by filtration (Whatman 0.45µm filter paper) using several volumes of ultrapure water to rinse and clean the silica samples. Filter papers were placed in petri-dishes in an incubator to dry. Collected silica was then weighed.

2.3 PDMPO fluorescence microscopy

Silica was immersed in 20mM PIPES buffer at pH7 adjusted with dilute NaOH (Acros Organics, Mw 302.35) with 0.125µM PDMPO (LysoSensor Yellow/blue DND-160 1mM in DMSO). After 24h incubation 50µL of the silica/PDMPO preparation was added to a cavity slide, covered with a cover slip and viewed using an Olympus BX50 fitted with a BXFLA fluorescent attachment using a U-MWU filter cube (Ex: 333-385nm; Em: 400-700 nm). A ColourView III digital camera (OSIS FireWire Camera 3.0 digitizer) was used to capture images in conjunction with CELL* Imaging software (Olympus Cell* family, Olympus Soft Imaging solutions GmbH 3.0).

2.4 Preparation of plant tissues for NanoSIMS

Small sections of horsetail (<1mm thickness) were cut by hand with a scalpel and fixed in 0.1M Na-cacodylate buffer (pH 7.4) with 3% glutaraldehyde. After fixation, samples were dehydrated in a graded ethanol series and infiltrated with increasing concentrations of LR White resin in ethanol. After polymerization, thin sections (1µm) were cut on a microtome with a diamond knife, placed onto a droplet of water on platinum-coated Thermanox

coverslips and stretched flat on a hotplate. Sections were coated with 10nm of platinum to avoid charging in the NanoSIMS.

2.5 NanoSIMS

High resolution SIMS analysis was carried out on a Cameca NanoSIMS 50 using a 16keV Cs^+ ion beam focused to approximately 100nm with a beam current of 1.2-1.4 pA. Negative secondary ions generated during this process were analyzed according to their mass to charge ratio using a double focusing mass spectrometer. The five detectors were precisely tuned using standards of Si and GaP to detect $^{12}C^-$, $^{12}C^{14}N^-$, $^{28}Si^-$, $^{31}P^{12}C^-$ and $^{32}S^-$ taking care to avoid mass interferences. The ion-induced secondary electron signal was also detected. For each area a dose of 1 x 10^{17} Cs^+ ions cm^2 was implanted by continuously scanning a large defocused beam to remove the platinum coating and maximize signal intensity. Dwell times were 10ms per pixel and for each region of interest.

2.6 Callose immunofluorescence

Identification of callose by immunofluorescence and fluorescence microscopy was carried out according to Pendle and Benitez-Alfonso (2015) [10] and briefly described herein. Small sections of horsetail tissues (<1mm thickness) were cut by hand with a scalpel, fixed and the cellulose in cell walls digested using 1% cellulase (Onozuka R-10, Yakult Pharm. Japan). Callose detection was performed on the extracted digested tissue using a (1-3)-β-glucan antibody (1:40; Biosupplies) and a secondary anti-mouse IgG-FITC antibody (1:40). Finally we used a Hoechst 33258 DNA counterstain and samples were mounted on glass slides and cover slipped. Tissue sections were viewed with a Zeiss Axioplan microscope (Blue Filter

Cube #487910; Ex: 450-490nm; Em: 515-565 nm) and images were captured using a Zeiss Axiocam MRc5 digital camera.

3. Results and Discussion

3.1. Si-deficient horsetail succumbed to biotic stressors after 10 weeks of healthy growth

Horsetail (*Equisetum* sp.) is known to accumulate silica in its tissues [11]. However we have shown that it is not required for the growth of healthy plants [7].

While growing horsetail (*E. arvense*) for an investigation into the reversibility of biological silicification, we made a novel observation in relation to the resistance of horsetail to biotic stressors. Hydroponic culture in 1/6th MS under Si-replete (2mM) or Si-deficient (12μM) conditions (see Section 2) resulted in healthy looking horsetail plants, with the only difference being that plants grown in the presence of added silicon (4 plants) were rough to the touch, which we assumed reflected the deposition of silica in their tissues. After 10 weeks of apparently healthy growth, a change was observed in the turgor, which was reduced, and the colour, which became paler, of horsetail plants growing under Si-deficient conditions (4 plants) and these changes were coincident with visible signs of fungal infection in all 4 plants (Figure 1). These observations are in agreement with what was previously shown in the literature, i.e. that Si-deficient horsetail had fragile, weak stems which subsequently withered, while Si-supplemented *Equisetum* did not [12]. Within 2 weeks, the infected areas were completely necrotic. Notably, this infection did not spread to horsetail plants grown in Si-replete conditions, despite the plants from different treatments being immediately adjacent to each other. Herein was evidence of the apparent benefit of silicon in protecting against fungal infection in horsetail. We endeavoured thereafter to establish how this apparently complete

protection against the development of fungal infection was afforded by investigating silica deposition in tissues of resistant plants using complementary imaging techniques.

3.2. NanoSIMS analysis of silica in horsetail tissues

The use of high-resolution secondary ion mass spectrometry (NanoSIMS) in plant biology couples high spatial resolution with sensitivity. Despite the complicated sample preparation protocol, this technique has been used to understand the distribution of several elements, including Si, in plant tissues [13,14].We used NanoSIMS (which identifies silica as $^{28}Si^{-}$ and hereafter will be referred to as silica) and fluorescence microscopy to map the exact location of silica in horsetail tissues. In particular we wanted to check for the presence of a silica-layer in horsetail tissue, since it is reported that one of the protective effects of silicon against pathogens is the formation of an "armour" providing mechanical shielding of cells [4]. This barrier is formed by the association of silica with cell wall components [15–17]. A previous study in the literature investigated the distribution of silica in horsetail using Raman imaging and highlighted its occurrence in the knobs and in a thin layer below the cuticle [18]. Our NanoSIMS analysis confirms these results and provides new, important data on the distribution of silica in horsetail tissues.

NanoSIMS was effective in identifying silica in leaves (highly reduced in size and connate laterally, thereby forming a protective sheath around stem nodes with the intercalary meristem [19]), branches and stems of Si-replete plants. Towards the edges of the leaf cross-sections (Figure 2A), silica was observed as a single layer on the epidermis of the inner leaf side facing the stem node (hereby referred to as inner epidermis for simplicity) and as a double layer on the epidermis of the outer leaf side facing the exterior (outer epidermis; Figure 2B and 2C). Both deposits appeared as continuous layers of silica, with the outermost silica layer being associated with the cuticle (as previously reported [18]) and the inner one appearing to

be associated with the cell wall. Away from the leaf edges and towards the broader central region of the cross-section (Figure 2D), the layer of silica associated with the outer epidermis was significantly thicker and appeared as a single diffuse layer incorporating, it would appear, the cell wall and cuticle (Figures 2E and 2F). It is noteworthy that NanoSIMS only identified silica in the cuticle/cell wall of leaf epidermal cells; silica was not observed associated with cell layers below the leaf epidermis (e.g. plasma membrane).

NanoSIMS was also performed on the stem, which is characterized by alternating furrows and ridges (with the ridges corresponding to the "knobs" described in [18]) (Figures 3A and 3D). A double layer of silica, sandwiching a distinct organic matrix (as identified by the clear C/N map), was observed in the furrow region of the stem (Figure 3A). Epidermal cells immediately adjacent to the furrow region also showed this distinctive double-layer of silica (Figure 4), similar, if not identical in appearance, to that of the edges of the outer leaf epidermis (Figures 2B and 2C). Numerous silica structures, either singular or in clusters (papilla-like), were observed projecting from the silica-cuticle layer (Figures 3B and 3C). A thick and apparently single layer of silica was observed in the sclerenchyma tissue (mainly composed of mixed-linkage glucans; [20]) which constitutes the stem ridge (Figures 3E and 3F). This heavily silicified region resembled in some ways the diffuse deposition of silica that was also seen in the central region of the leaf outer epidermis (Figures 2E and 2F). As with the leaf, silica deposition was not identified in the underlying non-epidermal tissues of the stem and it is also worth noting that silica was not associated with cell nuclei.

There was a single layer of silica associated with the cuticle of the branch epidermis (Figure 5A) and this single layer included regular papilla-like projections (Figures 5B and 5C). Intriguingly, a single silica layer was also observed associated with what appeared as an internal cell layer (Figure 5D) and, if confirmed, this is the first such observation by

NanoSIMS of a silicified non-epidermal cell layer in horsetail. This could be a silicified inner cell layer, or it may be an epidermis that has yet to unfurl.

3.3 Extraction of silica from horsetail tissues and imaging of their fine cellular details with PDMPO

Further evidence of silicification of horsetail grown under Si-replete conditions (note there was no silica to image in plants grown under Si-deficient conditions) was obtained from silica extracted by microwave-assisted acid digestion of stem and leaf and viewed using the fluor PDMPO [7] and fluorescence microscopy (Figure 6). These spectacular images confirmed that which was suggested by NanoSIMS (Figures 2-5), i.e. that the silicification of the silica-cuticle of the upper epidermis was continuous; a layer of silica, approximately 1µm thick that was continuous from the basal stem all the way to the leaf edge. Here we are describing a silica barrier associated with the cuticle, extending to the cell wall of the outer epidermis, and not silica 'phytoliths'. Numerous heavily silicified structures, from single silica projections to papilla-like structures, pores and stomata (Figure 6A and B), were observed within the silica barrier. The silicified stomata showed levels of silicification that appeared to mirror their developmental stage and included such fine details as their radial fibres (the "radiating ridges" described in 1973 [21]) and the stomatal pore (Figure 6B and inset). The silica extracts also showed cells whose cell walls appeared to be fully silicified (Figure 6C), cells which were in the process of division, plasmodesmata between adjacent cells [7] and, significantly, intracellular, usually spherical deposits, which resembled vesicles (Figure 6D). We know from NanoSIMS that the latter were not silicified nuclei (Figure 3A).

Imaging of extracted silica using PDMPO and fluorescence microscopy revealed the extent of biological silicification in a silica accumulator such as horsetail. It has also shown the intricate details of biogenic silica deposition including spectacularly the undulating structures of plant

cell walls, the different stages of cell cytokinesis and the individual steps in the differentiation and maturation of stomata. All of these structures and commensurate cellular processes exist and function in the absence of silicification and therefore, natural selection informs us, that all of them are equally effective as silicified isoforms.

3.4 Immunodetection of callose and its co-localization with silica

The 'Holy Grail' of biological silicification research is to identify the link between the organic biochemistry of silicified structures and the inorganic chemistry of biogenic silica precipitation and deposition. We have proposed that the β-1,3 glucan, callose, and its biochemical machinery is intimately involved in biological silicification in horsetail and other biota [7,8,22]. In *in vitro* experiments, callose was shown to trigger the precipitation of amorphous silica from an undersaturated silicic acid solution [7]. Further support for callose in templating silica deposition was demonstrated in the non-Si accumulator *Arabidopsis thaliana* (see Section 1) [8]. Herein we have used callose immunofluorescence [7] to further support this contention (Figure 7). We observed positive callose fluorescence which could be attributed to, (i) silicified projections, possibly papilla-like structures at the epidermis (Figures 7A-7B), (ii) the cuticle of the epidermis, (iii) punctate possibly intracellular deposits (Figures 7C-D), and (iv) especially associated with stomata (Figure 7E-7F). Particularly well defined was the callose-positive signal observed at the level of guard cells in stomata (Figure 7F and inset). The association of callose with guard cells was proven in both *Beta vulgaris* (in both young and mature guard cells) [23] and in the fern *Asplenium nidus* [24]. The association of callose with stomata in horsetail may be related to newly formed guard cells, but also to specific mechanical functions in the cell walls of more mature guard cells. Guard cells are specialized cell types whose walls need to withstand continuous cycles of closure and opening. Interestingly stronger enzyme solutions are needed to make protoplasts from guard

cells [23] (and references therein). This finding suggests that the composition of the guard cell wall and the structural arrangement of polysaccharides therein must enable plasticity and mechanical resistance to expansion/contraction. Callose is in this respect an ideal component in reinforcing the cell wall of guard cells. Silica may contribute to this cell wall strengthening effect, but it must do so while ensuring a certain degree of flexibility to the walls. Alternatively (or additionally), silica and callose may play a synergistic role in restricting the symplastic connectivity (to avoid leaking of molecular determinants, e.g. for stomatal patterning, to neighbouring cells) during the differentiation of cells. Callose was already shown to be important to restrict the symplastic movement of stomatal patterning regulators [25]. The role of callose in such processes, combined with its biochemistry and physico-chemical features [22], are inevitably triggering biosilicification in horsetail (provided the critical $Si(OH)_4$ concentration is available, see below).

3.5 Biogenic silica and callose: a mechanical and biochemical defence system in horsetail

We have shown that the epidermal surface of horsetail cultured in a Si-replete medium is heavily silicified and this silica barrier is continuous from the stem to the leaf and branches. It is probable that such a complete barrier of amorphous biogenic silica is impenetrable by fungal haustoria. In this respect it is worth mentioning that the application of silica gel to rice reduced the frequency of leaf appressorial penetration of *Magnaporthe oryzae* [26], a finding pointing to a silica physical barrier. Silica has been shown to form a cuticle-embedded layer in epidermal cells which makes them less susceptible to pathogen penetration (recently reviewed by [3]). Even potentially weaker points of entry through the epidermis such as pores, stomata and paracellular routes are shown herein to be protected by extensive silicification (Figure 6A and B). In the example herein, the high concentration of $Si(OH)_4$ present in culture media (2mM) resulted in the formation of a complete silica barrier at the

epidermis. The presence of this barrier was an apparent deterrent against fungal attack. Conversely, a Si-deficient culture medium (12μM) was not sufficient to result in the deposition of silica in horsetail tissues and this may explain the higher susceptibility of these plants to fungal infection. This last point is critical in that it demonstrates that even an infinite supply of $Si(OH)_4$ at a concentration of 12μM was not sufficient, at any point over a 12 week culture period, to support a super-saturated (>2mM) concentration of $Si(OH)_4$ in horsetail xylem. In other words, horsetail showed insufficient capacity to take up $Si(OH)_4$ from the culture medium and concentrate it in its tissues to a degree which could support subsequent silica deposition. This strongly suggests that there will be an as yet unknown critical concentration of medium (soil water) $Si(OH)_4$ below which horsetail will not deposit silica in its tissues. We might call this critical concentration, $[Si(OH)_4]_{Crit}$, and recognise that this value will be plant or species-specific and that it is most probably related to plant physiology. Above this critical concentration, while silica will be deposited, the extent and degree of silica deposition will vary according to the availability of $Si(OH)_4$ and horsetail may still be prone to fungal infection. For example, an incomplete barrier of silica at the epidermis might allow limited penetration by e.g. fungal haustoria (Figure 8). The latter might be damaged by silica present in the epidermis and the pathogen-mediated hyper-sensitive reaction (HR) initiated [27]. One aspect of HR is the induction of callose synthesis and its transport to sites of damage-recognition such as the halo surrounding the invading haustorium and papillae at the surface of the epidermis. The deposition of callose at such sites will be coincident with enhanced silica deposition and thus providing a second and important line of defence against further fungal infection (Figure 8). The synergy between callose and silica in horsetail is therefore even more striking under conditions of biotic stress. Our model of the presence of a first, biochemical callose-mediated line of defence and a second, adventitious callose-catalysed silica barrier is reminiscent of what was observed in French bean in 1985 [28]: in

that study the deposition of phenolics was proposed to be the first response, which then triggered the deposition of silica in Si-supplemented plants. It should be noted, with respect to our model, that phenolics are often found associated with papillae, where callose is a ubiquitous component [29].

4. Conclusions

Using NanoSIMS, we have provided evidence for the existence of a continuous silica layer in horsetail grown under Si-replete conditions. Interestingly, the silica layer is double in specific regions, for example, in the epidermis of the outer leaf side facing the exterior and in the stem furrows. We have shown that silica and callose co-localize in horsetail tissues and we postulate the existence of a unique relationship between $Si(OH)_4$ and callose in providing protection against fungal infection in horsetail. This relationship is unlikely to be unique to horsetail or even known silica accumulators, as something similar has already been suggested for thale cress [8,30,31] which is not known as a silica accumulator. It is clear that a $[Si(OH)_4]_{Crit}$ in culture media or soil water is required for any plant to deposit silica in its tissues and future research should look to identify such plant-specific $[Si(OH)_4]_{Crit}$ and the detailed mechanisms of subsequent deposition of biogenic silica. The observations herein highlight the potential for biogenic silica to protect against fungal infection and perhaps especially in important crop plants which have been genetically modified to be silica accumulators.

Conflict of interest

The authors declare no conflict of interest.

Acknowledgements

CL and IS were in receipt of NERC studentships. P. Panagiotis and P. Livanos (Athens) are thanked for their help with callose immunofluorescence.

References

[1] H. Etesami, B.R. Jeong, Silicon (Si): Review and future prospects on the action mechanisms in alleviating biotic and abiotic stresses in plants, Ecotoxicol. Environ. Saf. 147 (2018) 881–896. doi:10.1016/j.ecoenv.2017.09.063.

[2] G. Heine, G. Tikum, W.J. Horst, Silicon nutrition of tomato and bitter gourd with special emphasis on silicon distribution in root fractions, J. Plant Nutr. Soil Sci. 168 (2005) 600–606. doi:10.1002/jpln.200420508.

[3] M. Wang, L. Gao, S. Dong, Y. Sun, Q. Shen, S. Guo, Role of Silicon on Plant–Pathogen Interactions, Front. Plant Sci. 8 (2017). doi:10.3389/fpls.2017.00701.

[4] O.L. Reynolds, M.P. Padula, R. Zeng, G.M. Gurr, Silicon: Potential to Promote Direct and Indirect Effects on Plant Defense Against Arthropod Pests in Agriculture, Front. Plant Sci. 7 (2016) 744. doi:10.3389/fpls.2016.00744.

[5] S.C. Fry, B.H.W.A. Nesselrode, J.G. Miller, B.R. Mewburn, Mixed-linkage (1-->3,1-->4)-beta-D-glucan is a major hemicellulose of *Equisetum* (horsetail) cell walls, New Phytol. 179 (2008) 104–115. doi:10.1111/j.1469-8137.2008.02435.x.

[6] N. Kido, R. Yokoyama, T. Yamamoto, J. Furukawa, H. Iwai, S. Satoh, K. Nishitani, The matrix polysaccharide (1;3,1;4)-β-D-glucan is involved in silicon-dependent strengthening of rice cell wall, Plant Cell Physiol. 56 (2015) 268–276. doi:10.1093/pcp/pcu162.

[7] C. Law, C. Exley, New insight into silica deposition in horsetail (*Equisetum arvense*), BMC Plant Biol. 11 (2011) 112. doi:10.1186/1471-2229-11-112.

[8] T. Brugiére, C. Exley, Callose-associated silica deposition in *Arabidopsis*, J. Trace Elem. Med. Biol. Organ Soc. Miner. Trace Elem. GMS. 39 (2017) 86–90. doi:10.1016/j.jtemb.2016.08.005.

[9] H.A. Currie, C.C. Perry, Silica in Plants: Biological, Biochemical and Chemical Studies, Ann. Bot. 100 (2007) 1383–1389. doi:10.1093/aob/mcm247.

[10] A. Pendle, Y. Benitez-Alfonso, Immunofluorescence detection of callose deposition around plasmodesmata sites, Methods Mol. Biol. 1217 (2015) 95-104. doi: 10.1007/978-1-4939-1523-1_6.

[11] H.A. Currie, C.C. Perry, Chemical evidence for intrinsic "Si" within *Equisetum* cell walls, Phytochemistry. 70 (2009) 2089–2095. doi:10.1016/j.phytochem.2009.07.039.

[12] S. Yamanaka, K. Sato, F. Ito, S. Komatsubara, H. Ohata, K. Yoshino, Roles of silica and lignin in horsetail (*Equisetum hyemale*), with special reference to mechanical properties, J. Appl. Phys. 111 (2012) 044703. doi:10.1063/1.3688253.

[13] K.L. Moore, M. Schröder, Z. Wu, B.G.H. Martin, C.R. Hawes, S.P. McGrath, M.J. Hawkesford, J. Feng Ma, F.-J. Zhao, C.R.M. Grovenor, High-Resolution Secondary Ion Mass Spectrometry Reveals the Contrasting Subcellular Distribution of Arsenic and Silicon in Rice Roots, Plant Physiol. 156 (2011) 913–924. doi:10.1104/pp.111.173088.

[14] K.L. Moore, Y. Chen, A.M.L. van de Meene, L. Hughes, W. Liu, T. Geraki, F. Mosselmans, S.P. McGrath, C. Grovenor, F.-J. Zhao, Combined NanoSIMS and synchrotron X-ray fluorescence reveal distinct cellular and subcellular distribution patterns of trace elements in rice tissues, New Phytol. 201 (2014) 104–115. doi:10.1111/nph.12497.

[15] G. Guerriero, J.-F. Hausman, S. Legay, Silicon and the Plant Extracellular Matrix, Front. Plant Sci. 7 (2016) 463. doi:10.3389/fpls.2016.00463.

[16] M. Luyckx, J.-F. Hausman, S. Lutts, G. Guerriero, Silicon and Plants: Current Knowledge and Technological Perspectives, Front. Plant Sci. 8 (2017). doi:10.3389/fpls.2017.00411.

[17] M. Luyckx, J.-F. Hausman, S. Lutts, G. Guerriero, Impact of Silicon in Plant Biomass Production: Focus on Bast Fibres, Hypotheses, and Perspectives, Plants Basel Switz. 6 (2017). doi:10.3390/plants6030037.

[18] N. Gierlinger, L. Sapei, O. Paris, Insights into the chemical composition of *Equisetum hyemale* by high resolution Raman imaging, Planta. 227 (2008) 969–980. doi:10.1007/s00425-007-0671-3.

[19] A. Vasco, R.C. Moran, B.A. Ambrose, The evolution, morphology, and development of fern leaves, Front. Plant Sci. 4 (2013). doi:10.3389/fpls.2013.00345.

[20] O. Leroux, J.P. Knox, B. Masschaele, A. Bagniewska-Zadworna, S.E. Marcus, M. Claeys, L. van Hoorebeke, R.L.L. Viane, An extensin-rich matrix lines the carinal canals in *Equisetum ramosissimum*, which may function as water-conducting channels, Ann. Bot. 108 (2011) 307–319. doi:10.1093/aob/mcr161.

[21] P. Dayanandan, P. B. Kaufman, Stomata in *Equisetum*, Can. J. Bot. 51 (1973) 1555-1564. doi:10.1139/b73-198.

[22] C. Exley, A possible mechanism of biological silicification in plants, Front. Plant Sci. 6 (2015). doi:10.3389/fpls.2015.00853.

[23] A. Majewska-Sawka, A. Münster, M.I. Rodríguez-García, Guard cell wall: immunocytochemical detection of polysaccharide components, J. Exp. Bot. 53 (2002) 1067–1079. doi:10.1093/jexbot/53.371.1067.

[24] P. Apostolakos, P. Livanos, T.L. Nikolakopoulou, B. Galatis, The role of callose in guard-cell wall differentiation and stomatal pore formation in the fern *Asplenium nidus*, Ann. Bot. 104 (2009) 1373–1387. doi:10.1093/aob/mcp255.

[25] J.M. Guseman, J.S. Lee, N.L. Bogenschutz, K.M. Peterson, R.E. Virata, B. Xie, M.M. Kanaoka, Z. Hong, K.U. Torii, Dysregulation of cell-to-cell connectivity and stomatal patterning by loss-of-function mutation in *Arabidopsis CHORUS* (*GLUCAN SYNTHASE-LIKE 8*), Development. 137 (2010) 1731–1741. doi:10.1242/dev.049197.

[26] T. Hayasaka, H. Fujii, K. Ishiguro, The Role of Silicon in Preventing Appressorial Penetration by the Rice Blast Fungus, Phytopathology. 98 (2008) 1038–1044. doi:10.1094/PHYTO-98-9-1038.

[27] M. Grant, J. Mansfield, Early events in host-pathogen interactions, Curr. Opin. Plant Biol. 2 (1999) 312–319. doi:10.1016/S1369-5266(99)80055-7.

[28] M.A. Stumpf, M.C. Heath, Cytological studies of the interactions between the cowpea rust fungus and silicon-depleted French bean plants, Physiol. Plant Pathol. 27 (1985) 369–385. doi:10.1016/0048-4059(85)90049-9.

[29] C.A. Voigt, Callose-mediated resistance to pathogenic intruders in plant defense-related papillae, Front. Plant Sci. 5 (2014). doi:10.3389/fpls.2014.00168.

[30] F. Fauteux, F. Chain, F. Belzile, J.G. Menzies, R.R. Bélanger, The protective role of silicon in the *Arabidopsis*-powdery mildew pathosystem, Proc. Natl. Acad. Sci. U. S. A. 103 (2006) 17554–17559. doi:10.1073/pnas.0606330103.

[31] J. Vivancos, C. Labbé, J.G. Menzies, R.R. Bélanger, Silicon-mediated resistance of *Arabidopsis* against powdery mildew involves mechanisms other than the salicylic acid (SA)-dependent defence pathway, Mol. Plant Pathol. 16 (2015) 572–582. doi:10.1111/mpp.12213.

Figure legends

Figure 1: Susceptibility to fungal infection of horsetail grown under Si-deficient conditions. A) Horsetail grown under Si-replete condition. B) Horsetail grown under Si-deficient condition showing signs of fungal infection though only after 10 weeks of healthy growth. Arrows in the inset indicate fungal mycelia.

Figure 2: NanoSIMS image of horsetail leaves. A) The upper panel shows the optical image of the leaf section analysed by NanoSIMS with the red square indicating the location of the NanoSIMS analysis at the edge of the leaf, Scale bar = 100µm. B) The lower left panel shows the NanoSIMS ion signals from this region as a colour merge image with $^{28}Si^-$ in red, $^{12}C^{14}N^-$ in green and $^{31}P^{12}C^-$ in blue, scale bar = 15µm. C) The lower right panel shows $^{28}Si^-$ in red (the arrow indicates the Si double layer) and in grey the secondary electron (SE) image. D) The upper panel shows the optical image of the central portion of the leaf outer epidermis analysed by NanoSIMS with the red square indicating the location of the NanoSIMS analysis at the edge of the leaf, scale bar = 15µm. E) The lower left panel shows the NanoSIMS ion signals from this region as a colour merge image with $^{28}Si^-$ in red, $^{12}C^{14}N^-$ in green and $^{31}P^{12}C^-$ in blue, scale bar = 15µm. F) The lower right panel shows $^{28}Si^-$ in red (the arrow indicates the thick Si associated with the cuticle and cell wall) and in grey the secondary electron (SE) image.

Figure 3: NanoSIMS image of horsetail stem. A) The upper panel shows the optical image of the portion of the stem furrow analysed by NanoSIMS with the red square indicating the location of the NanoSIMS analysis, scale bar = 100µm. B) The lower left panel shows the NanoSIMS ion signals from this region as a colour merge image with $^{28}Si^-$ in red, $^{12}C^{14}N^-$ in green and $^{31}P^{12}C^-$ in blue (the arrow indicates a cell nucleus), scale bar = 15µm. C) The lower right panel shows $^{28}Si^-$ in red (the arrows indicate the Si double layer and the papilla-like projections) and in grey the secondary electron (SE) image. D) The upper panel shows the optical image of the portion of the stem ridge analysed by NanoSIMS with the red square

indicating the location of the NanoSIMS analysis, scale bar = 100µm. E) The lower left panel shows the NanoSIMS ion signals from this region as a colour merge image with $^{28}Si^-$ in red, $^{12}C^{14}N^-$ in green and $^{31}P^{12}C^-$ in blue, scale bar = 15µm. F) The lower right panel shows $^{28}Si^-$ in red (the arrow indicates the thick Si layer associated with the sclerenchyma) and in grey the secondary electron (SE) image.

Figure 4: NanoSIMS image of the stem region adjacent to a stem furrow. A very clear Si double layer (red) with an 'organic filling' identified by the $^{12}C^{14}N^-$ map (green) is associated with the epidermis. Scale bar = 15µm.

Figure 5: NanoSIMS image of horsetail branch. A) Optical image of the stem branch with red squares indicating the positions of NanoSIMS analysis. In all images on the left, $^{28}Si^-$ is shown in red, $^{12}C^{14}N^-$ in green and $^{31}P^{12}C^-$ in blue, scale bar = 15µm. On the right, $^{28}Si^-$ is shown in red and in grey the secondary electron (SE) image. B) Outer branch portion with arrows indicating the Si layer and the papilla-like projections. C) Inner branch portion with the arrow indicating the thick Si layer associated with a silicified papilla-like projection. D) Inner cell layer of the stem branch with the arrow indicating the inner Si layer.

Figure 6: Biogenic silica deposition in horsetail stem and leaves following acid extraction and fluorescence imaging with PDMPO. A) Stomata and papillae-like projections on the stem epidermis (arrows). B) Clusters of silicified papillae-like projections on the leaf (arrows) and fine detail of a stoma showing the thickened ventral cell walls of guard cells (inset). C) Jigsaw puzzle-like silicified cell walls of the stem epidermal cells. D) Silicified vesicles/inner deposits in leaf epidermal cells (arrows).

Figure 7: Callose immunodetection in horsetail stem epidermis. Panels A and B indicate clusters of papillae-like projections. C and D indicate epidermal cells with vesicles reacting against the antibody (arrow). E and F show epidermal jigsaw puzzle-like cells and stomata.

The inset in F shows a detail of a stoma with fluorescence of the guard cells' ventral cell walls.

Figure 8: **Schematic model representing the double defence system against biotic stress in horsetail.** The three scenarios, i.e. Si-deficient ($<[Si(OH)_4]_{Crit}$), Si-sufficient ($\geq[Si(OH)_4]_{Crit}$) and Si-replete ($>>[Si(OH)_4]_{Crit}$), are depicted.

A

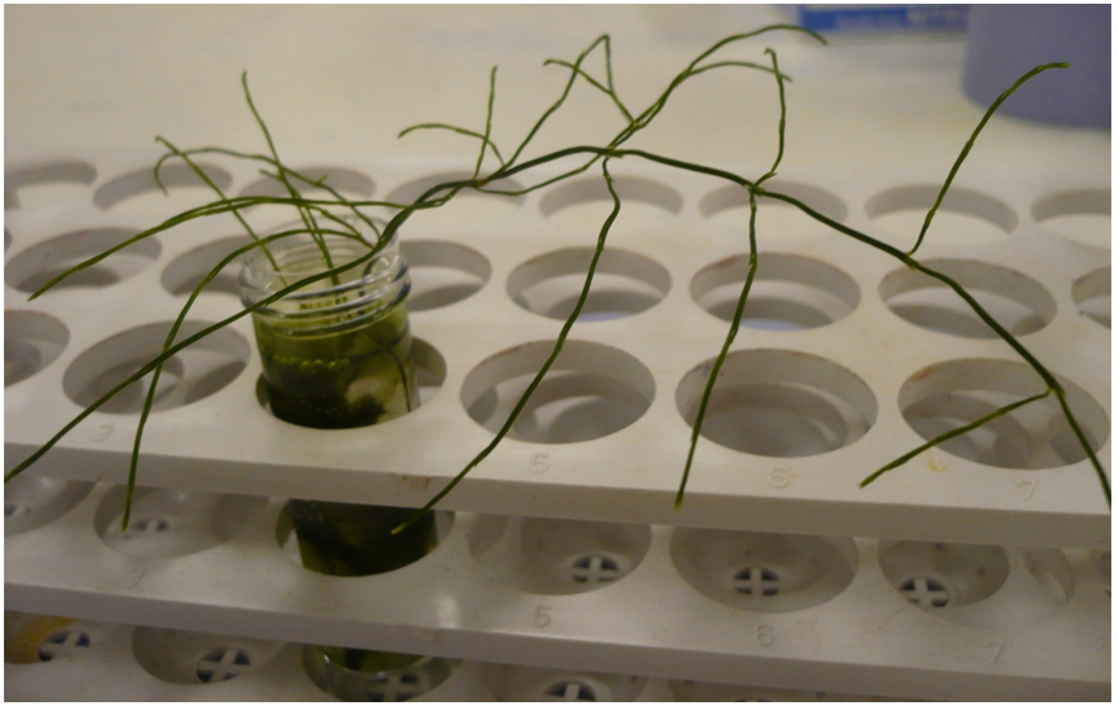

B

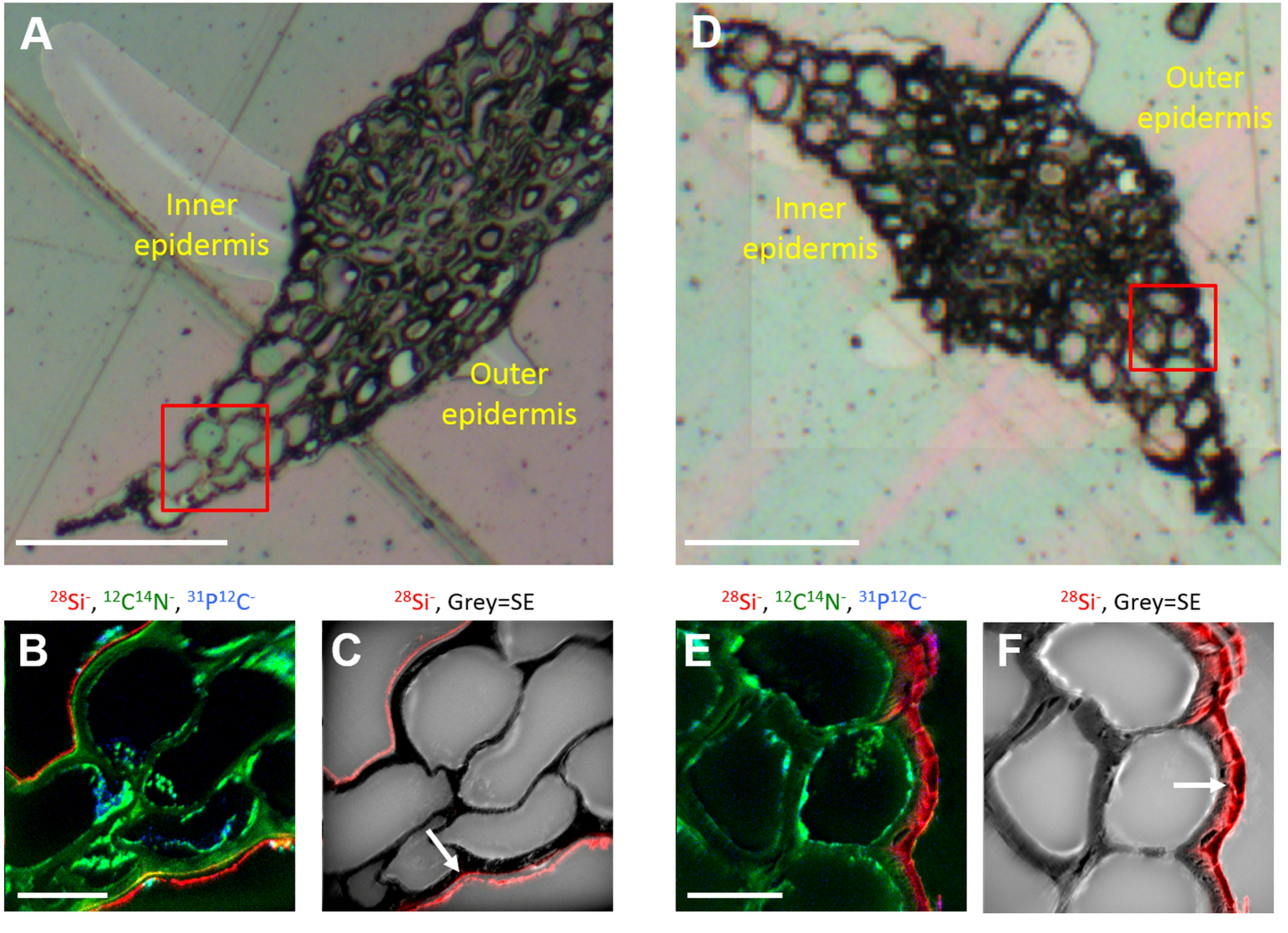
A
Inner epidermis
Outer epidermis
D
Outer epidermis
Inner epidermis
$^{28}Si^-$, $^{12}C^{14}N^-$, $^{31}P^{12}C^-$
$^{28}Si^-$, Grey=SE
$^{28}Si^-$, $^{12}C^{14}N^-$, $^{31}P^{12}C^-$
$^{28}Si^-$, Grey=SE
B
C
E
F

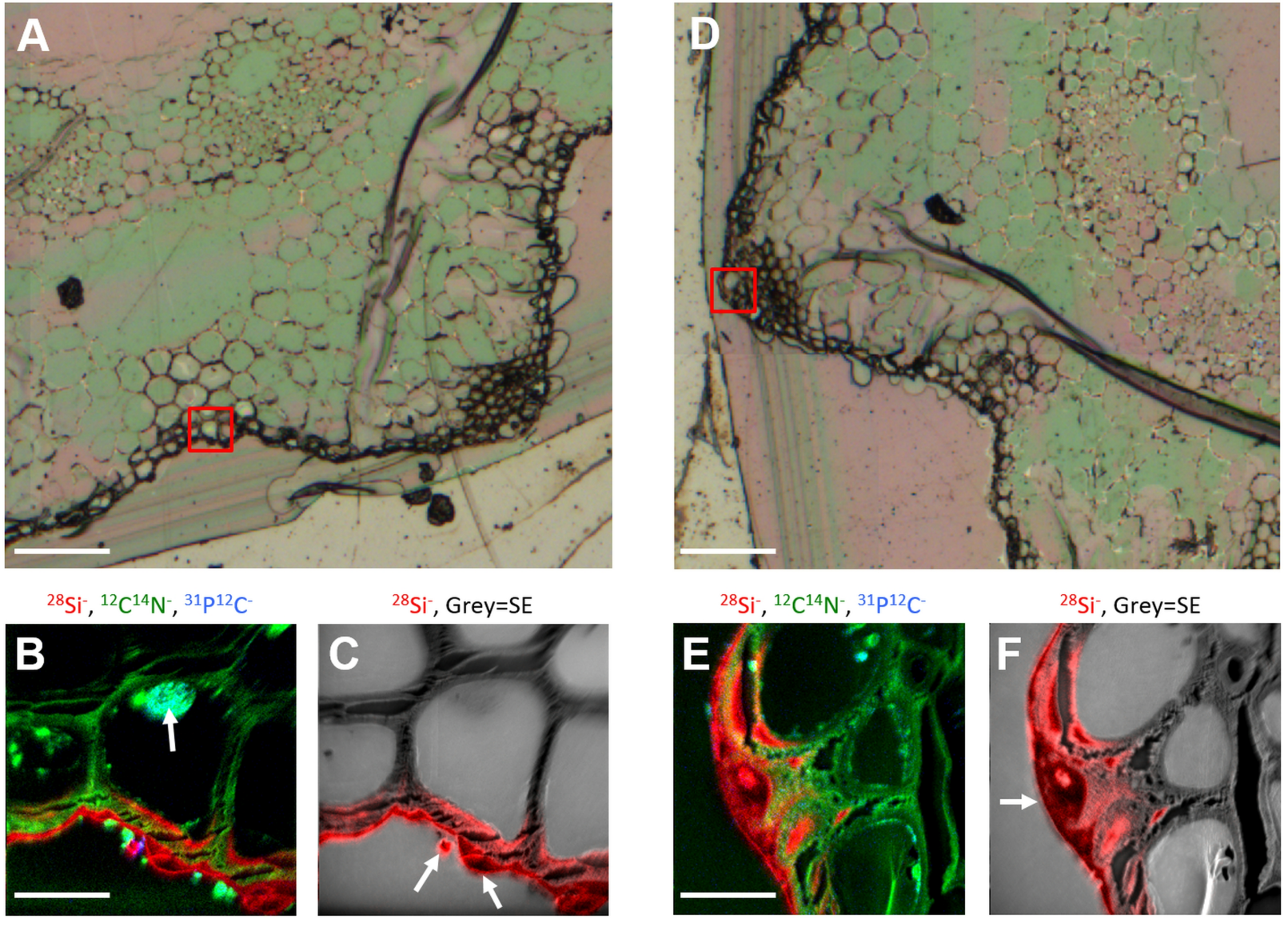
A
D
$^{28}Si^-$, $^{12}C^{14}N^-$, $^{31}P^{12}C^-$
$^{28}Si^-$, Grey=SE
$^{28}Si^-$, $^{12}C^{14}N^-$, $^{31}P^{12}C^-$
$^{28}Si^-$, Grey=SE
B
C
E
F

$^{28}Si^{-}$, $^{12}C^{14}N^{-}$, $^{31}P^{12}C^{-}$

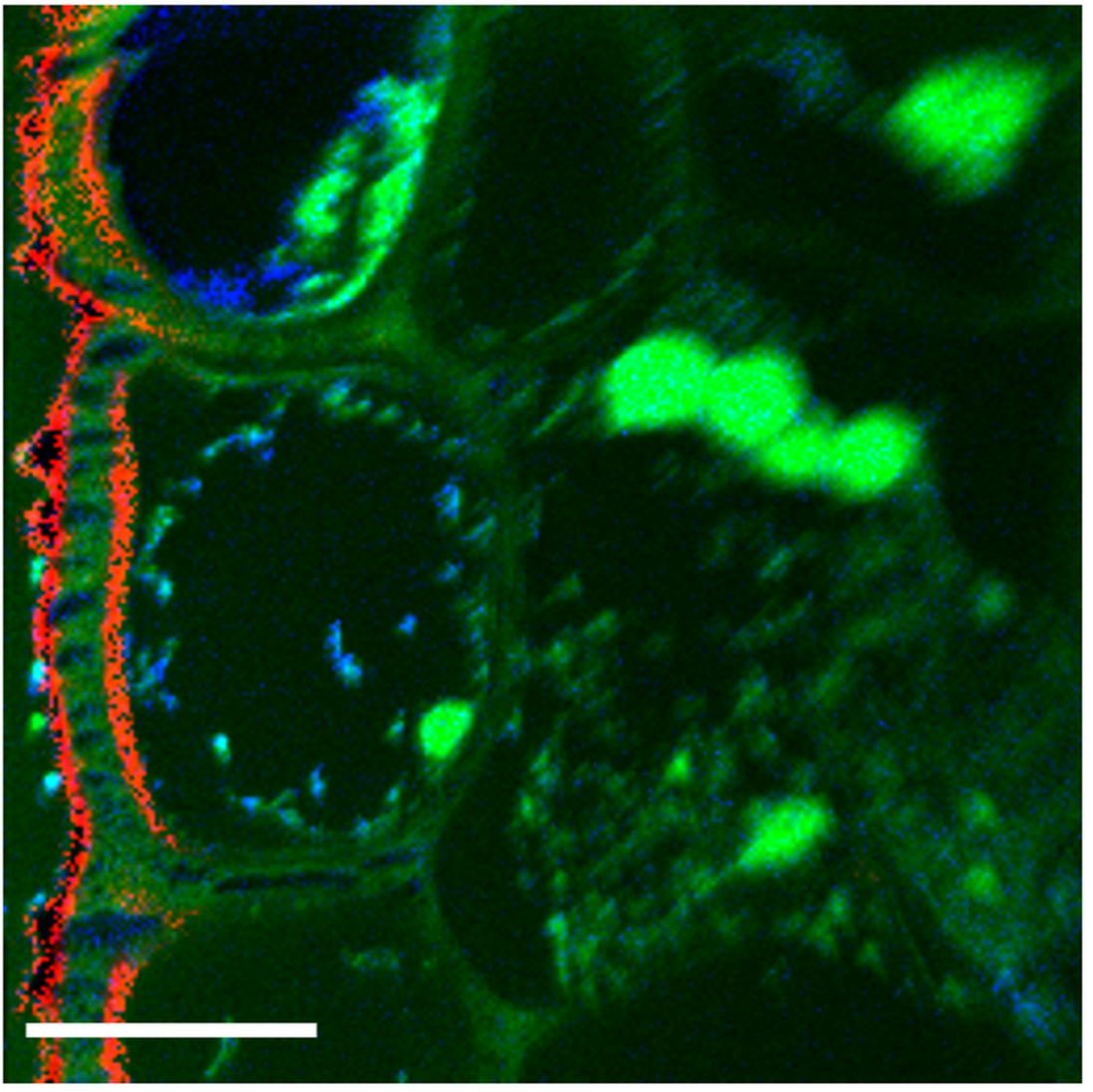

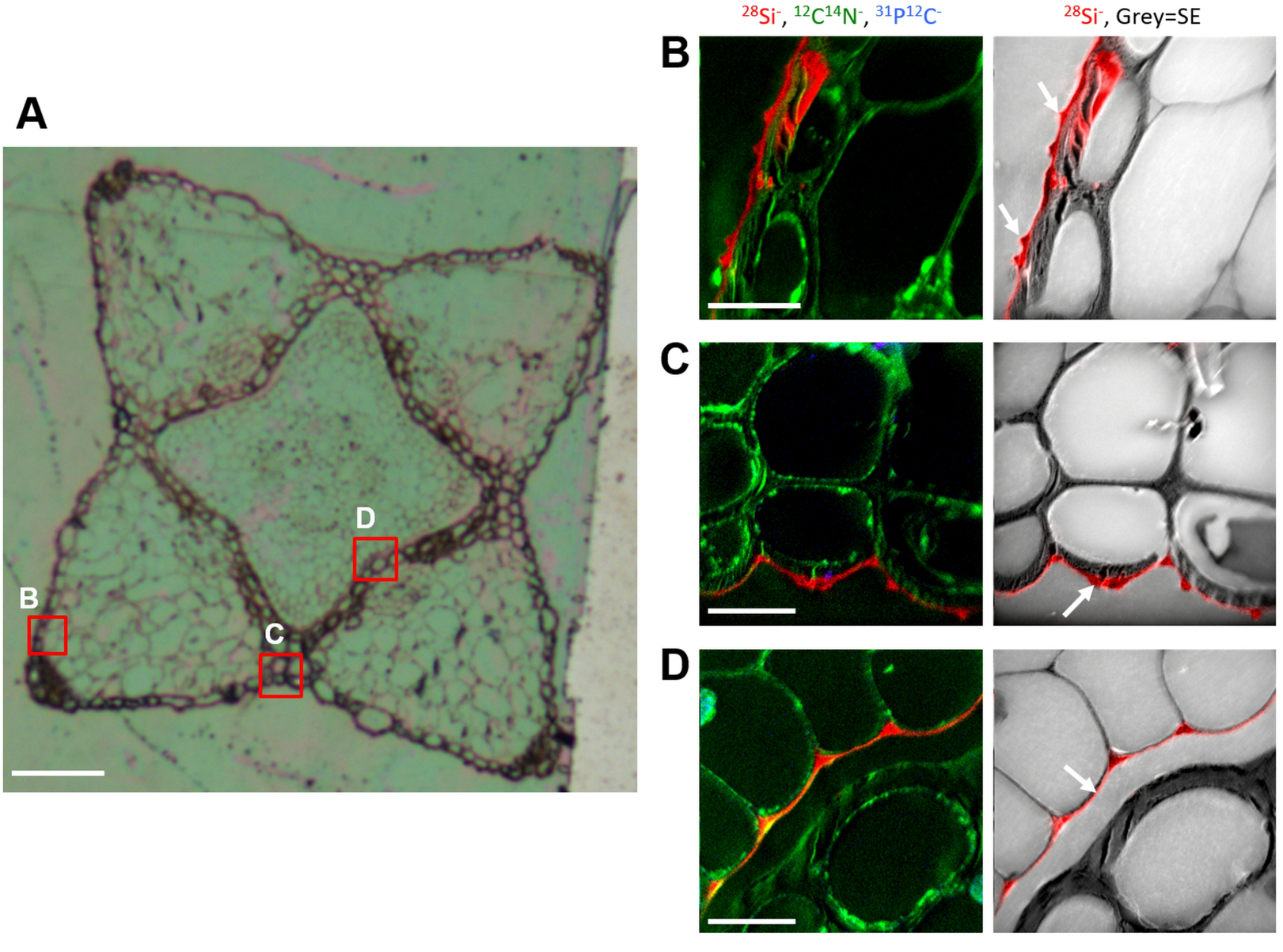
A
B
C
D
$^{28}Si^-$, $^{12}C^{14}N^-$, $^{31}P^{12}C^-$
$^{28}Si^-$, Grey=SE
B
C
D

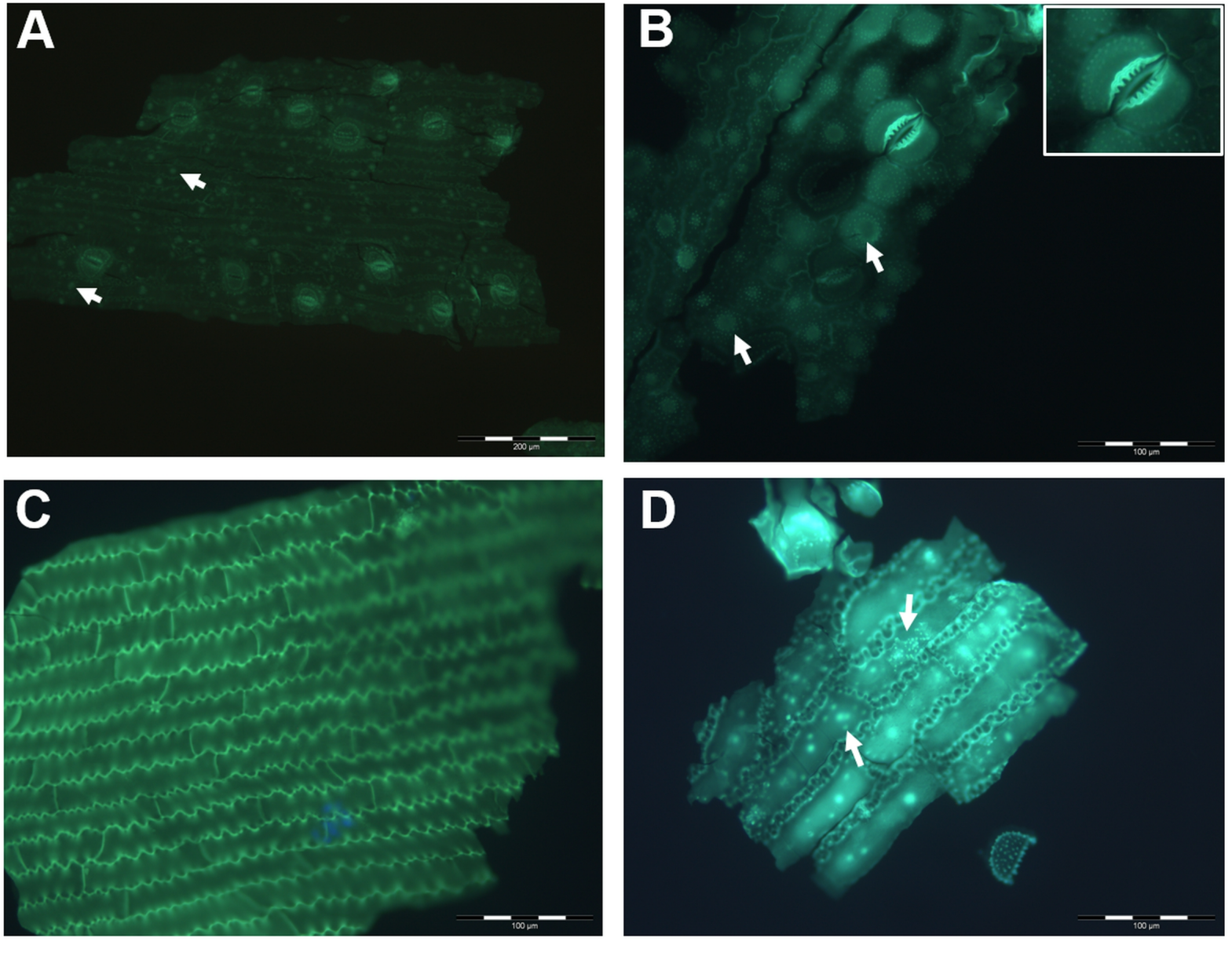
A
200 µm
B
100 µm
C
100 µm
D
100 µm

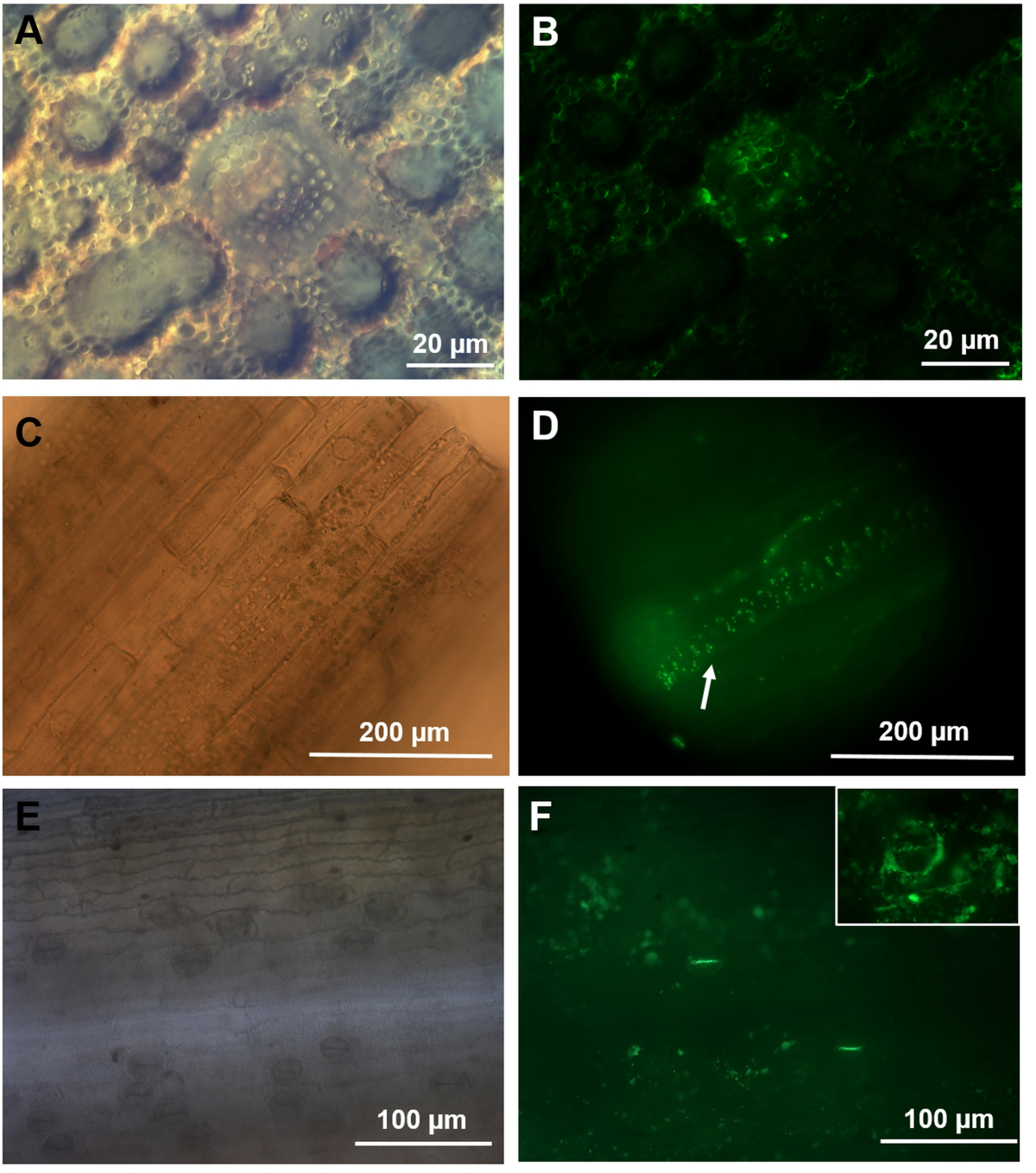
A
20 µm
B
20 µm
C
200 µm
D
200 µm
E
100 µm
F
100 µm

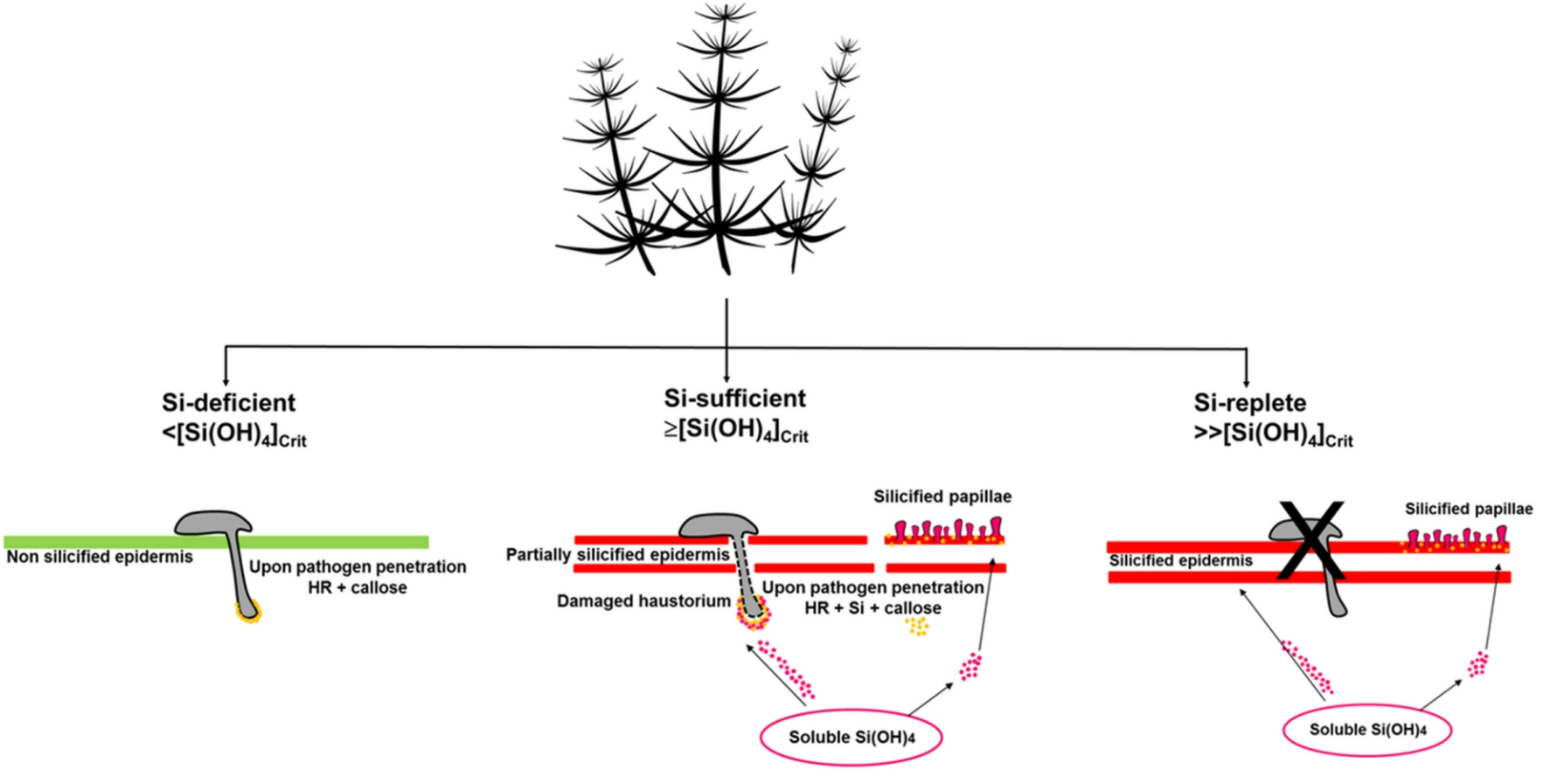
Si-deficient
<[Si(OH)4]Crit
Si-sufficient
≥[Si(OH)4]Crit
Si-replete
>>[Si(OH)4]Crit
Non silicified epidermis
Upon pathogen penetration
HR + callose
Silicified papillae
Partially silicified epidermis
Damaged haustorium
Upon pathogen penetration
HR + Si + callose
Soluble Si(OH)4
Silicified papillae
Silicified epidermis
Soluble Si(OH)4

Competing interests

The authors declare that they have no competing interests.